

# Spinnability of Low-Substituted Hydroxyethylcellulose Sodium Hydroxide Aqueous Solutions

Dongmei Li,<sup>1,2</sup> Xingping Zhou,<sup>3</sup> Yang Jinglan,<sup>1</sup> Fangfang Yu,<sup>1</sup> Xiaqin Wang<sup>1,2</sup>

<sup>1</sup>State Key Laboratory for Modification of Chemical Fibers and Polymer Materials, College of Materials Science and Engineering, Donghua University, North Remin Road 2999, Shanghai 201620, People's Republic of China

<sup>2</sup>Key Laboratory of Science and Technology of Eco-Textile, Ministry of Education, North Remin Road 2999, Shanghai 201620, People's Republic of China

<sup>3</sup>College of Chemical Engineering and Biotechnology, Donghua University, North Remin Road 2999, Shanghai 201620, People's Republic of China

Received 27 November 2008; accepted 25 May 2009

DOI 10.1002/app.30876

Published online 26 March 2010 in Wiley InterScience (www.interscience.wiley.com).

**ABSTRACT:** Ethylene oxide was used to etherify alkali cellulose with a low substitution degree to replace carbon disulfide to generate cellulose xanthogenate by viscose technology. The resultant low-substituted hydroxyethylcellulose (LSHEC), with molar substitution of 0.49, was used to attempt to spin LSHEC fibers under spinning and coagulation conditions identical to those used for industrial rayon fibers. The spinnability of LSHEC was investigated by the variation of the storage modulus, loss modulus, and complex viscosity with the concentration of the LSHEC spinning solutions and temperature. It was found that the dissolution of LSHEC in sodium hydroxide aqueous solutions was an exothermic process, whereas the gelation of LSHEC was an endothermic process. Spinning

conditions, comprising the concentration of the spinning solutions and corresponding spinning temperatures, were derived from the gelation onset curve theoretically. Moreover, combinations of the concentration of the spinning solution and the temperature of the coagulation bath could be predicted by the gelation onset curve. Finally, LSHEC fibers were prepared under the spinning conditions based on the gelation onset curve. The as-spun LSHEC fibers had dry and wet tensile strengths of 1.59 and 0.47 cN/dtex, respectively, with a 0.30 ratio of the wet tensile strength to the dry tensile strength. © 2010 Wiley Periodicals, Inc. *J Appl Polym Sci* 117: 767–774, 2010

**Key words:** fibers; gelation; processing

## INTRODUCTION

Cellulose fibers, the most abundant renewable resource in nature, are honored as some of the green fibers of the 21st century with respect to environmental protection and petroleum consumption.<sup>1,2</sup> The physical and chemical properties of cellulose can be significantly tuned by derivatization. Cellulose derivatives have actually been widely used in many fields, such as modern coatings, biodegradable plastics, and separation membranes. However, the current cellulose fiber industry faces the tremendous challenge of economical and environmentally friendly chemical processing. Chemical processing of cellulose is difficult in general because this natural

polymer is neither meltable nor soluble in water or most organic solvents on account of its strong intermolecular and intramolecular hydrogen bonding and partially crystalline structures.<sup>3</sup> The production of regenerated cellulose fibers is based primarily on viscose technology established more than 100 years ago, which applies hazardous carbon disulfide (CS<sub>2</sub>) to generate a metastable soluble cellulose derivative, cellulose xanthogenate, as an intermediate. Cellulose xanthogenate is finally restored into the original cellulose during spinning. It has also been reported that cellulose fibers can be spun from a sodium hydroxide (NaOH)/urea aqueous solution directly.<sup>4</sup> The cuprammonium process is another classical route for manufacturing regenerated cellulose fibers, in which cellulose is converted into a soluble compound by combination with copper and ammonia. The cuprammonium process also faces environmental problems and therefore plays only a minor role in the current cellulose fiber industry.<sup>5</sup> Therefore, the development of alternative economical and environmentally friendly processes of regenerated cellulose fibers is still extremely desirable. Much attention has been paid to environmentally compatible lyocell and carbamate processes. The lyocell process uses *N*-methylmorpholine-*N*-oxide as the direct

Correspondence to: X. Wang (xqwang@dhu.edu.cn).

Contract grant sponsor: Central Specialized Research Fund for Universities (Donghua University), Specialized Research Fund for the Doctoral Program of Higher Education; contract grant number: 20060255008.

Contract grant sponsor: Program of Introducing Talents of Discipline to Universities; contract grant number: 111-2-04.

solvent of cellulose.<sup>6</sup> However, recycling this costly solvent really presents a great burden to manufacturers. The carbamate process employs cellulose carbamate for the manufacture of cellulose fibers instead of xanthogenate in the viscose process.<sup>7,8</sup> However, the carbamate process has not yet superseded the viscose process because of its high energy consumption.

Hydroxyethylcellulose is a well-known and widely used water-soluble polymer that is generally employed as a useful viscosifier with numerous applications.<sup>9</sup> We are motivated to establish a new process for cellulose fibers using low-substituted hydroxyethylcellulose (LSHEC) as the raw material. LSHEC is capable of fiber spinning, playing a role similar to that of cellulose xanthogenate in the viscose process, because LSHEC is soluble in NaOH aqueous solutions. The most evident advantage of the new process is that LSHEC fibers can be spun from viscose spinning devices. In viscose technology, cellulose is treated with a highly toxic chemical, CS<sub>2</sub>, to make it soluble in alkali. CS<sub>2</sub> is known to accelerate atherosclerosis and to increase the risk for cardiovascular diseases.<sup>10</sup> The new process uses ethylene oxide to etherify alkali cellulose with a low degree of substitution, which promotes the dissolution of LSHEC in NaOH aqueous solutions and coagulation from a coagulation bath. Ethylene oxide is an important industrial chemical often used as an intermediate in the production of ethylene glycol and other chemicals. Ethylene oxide is also widely used as a sterilant for foodstuffs and chemical supplies. The main difference between the viscose process and the new LSHEC process is that ethylene oxide is used to etherify alkali cellulose in the LSHEC process, whereas CS<sub>2</sub> is used to esterify alkali cellulose in the viscose process. Fortunately, the dry mechanical properties of LSHEC fibers are comparable to those of viscose rayon.<sup>4,11</sup> Therefore, the LSHEC process is rather promising as a partial or total replacement for the viscose process if the wet mechanical properties of LSHEC fibers, especially the wet tensile strength, meet those of viscose rayon via post intrafiber cross-linking used to diminish the excessive swelling of LSHEC fibers in water. In this research, the spinnability of LSHEC was investigated to figure out appropriate spinning and coagulation conditions as these conditions have a significant impact on the formation of LSHEC fibers.

## EXPERIMENTAL

### Materials

Alkali cellulose after ripening and cotton-type rayon staple fibers with an average length of 38 mm and a linear density of 1.67 dtex were kindly supplied by

Nanjing Chemical Fiber Co., Ltd. (Nanjing, China) and used as the starting cellulose. The composition of the alkali cellulose was 30%  $\alpha$ -cellulose, 17% NaOH, and 53% water. Ethylene oxide with a purity of greater than 99% was provided by Shanghai Air Water International Trade Co., Ltd. (Shanghai, China). Acetic anhydride, pyridine, and acetone were purchased from Shanghai Chemical Reagent Co., Ltd. (Shanghai, China).

### Preparation of LSHEC

The preparation of LSHEC was carried out as follows. Alkali cellulose [270 g with 81 g of  $\alpha$ -cellulose (0.5 mol)] was initially placed in a 3-L stainless steel autoclave equipped with a vacuum and a mechanical stirrer. Ethylene oxide (11 g, 0.25 mol) chilled with ice was added to the autoclave under vigorous stirring after a vacuum was applied, and the temperature of the autoclave was maintained at 25°C with a constant-temperature circulator. Then, the consumption of ethylene oxide was followed with a vacuumeter. The etherification of cellulose was stopped after the pressure inside the autoclave resumed nearly its original value before the addition of ethylene oxide after the reaction was stirred and maintained at 25°C for 1.5 h. The yield of LSHEC was 83.6%.

### Acetylation of LSHEC<sup>12</sup>

The etherified product was neutralized with a 0.1M HCl aqueous solution and washed with deionized water repeatedly. Then, LSHEC was collected via filtration and dried thoroughly before acetylation. Acetylation of LSHEC was carried out by the refluxing of LSHEC in an acetic anhydride/pyridine mixture. LSHEC (20 g), 100 mL of pyridine, and 50 mL of acetic anhydride were placed in a 500-mL flask and heated to reflux for 3 h. The product was isolated by precipitation into 2.0 L of deionized water and washed with a large amount of deionized water. Finally the product was further purified by reprecipitation from deionized water/acetone and then dried completely.

### Preparation of the LSHEC spinning solutions

A typical preparation of the spinning solutions was carried out as follows. The previously described etherified product (104.92 g) was weighed to prepare the spinning solution, which consisted of 34.21 g of LSHEC and 18.20 g of NaOH. Then, 17.80 g of NaOH and deionized water were added up to a total weight of 450 g. The dissolution of LSHEC was conducted at 20°C under vigorous stirring for 15 min. The LSHEC concentration was 7.6 wt % in the spinning solution, and the NaOH concentration was 8.0 wt %.

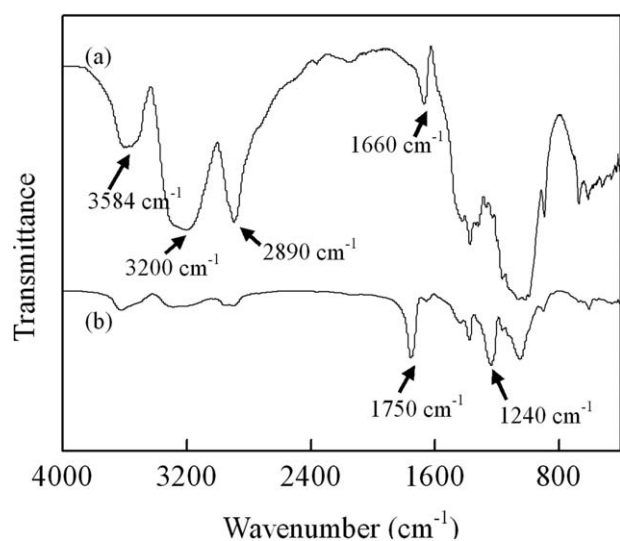


**Figure 1** FTIR spectra for (a) LSHEC and (b) acetylated LSHEC.

### Spinning of the LSHEC fibers

The spinning of the LSHEC fibers was conducted on a homebuilt wet-spinning machine. The spinning solution was first filtered and then allowed to flow into a spinneret to form filaments through control of the flow rate with a metering pump. The as-spun LSHEC fibers were coagulated from a coagulation bath comprising 10.55 wt %  $H_2SO_4$ , 20.31 wt %  $Na_2SO_4$ , 1.41 wt %  $ZnSO_4$ , and 67.73 wt % water, and then they were drawn in a hot water bath with a temperature of 50°C. Finally, the drawn fibers were washed with water and dried.

### Characterization

Dynamic rheology experiments were carried out on an ARES RFS rheometer (TA Instruments, New Castle, DE). A pair of parallel plates with a diameter of 50 mm and a gap of 1 mm was used for monitoring the modulus and viscosity evolution during the gelation of LSHEC. The measurement temperature was controlled within  $\pm 0.5^\circ C$ . The shear storage modulus ( $G'$ ), loss modulus ( $G''$ ), and complex viscosity ( $\eta^*$ ) were measured as a function of temperature. A degassed LSHEC spinning solution was heated to the desired temperature in the rheometer without shearing or oscillating. The dynamic temperature sweep was performed at a shear strain amplitude of 10% with an angular frequency of 1 rad/s within a linear viscoelastic region.

Fourier transform infrared (FTIR) spectra were recorded on a Nicolet 20sx-B infrared spectrometer (Nicolet Instrument Corp., Madison, WI). A total of 16 scans for each sample were taken with a resolution of  $2\text{ cm}^{-1}$ . Potassium bromide powder was used as a reference to produce a background spec-

trum.  $^1H$ -NMR spectra of LSHEC in  $CDCl_3$  were recorded on a Bruker AV 400 NMR spectrometer (Bruker Inc., Fallanden, Switzerland) in a proton noise decoupling mode at 40°C. Acetylation of LSHEC was accomplished before NMR analysis on the basis of a reported method.<sup>13</sup> Scanning electron microscopy (SEM) images were obtained with a JEOL JSM-5600 (Jeol, Ltd., Tokyo, Japan) operated at an accelerating voltage of 10 kV. X-ray powder diffraction (XRD) patterns were determined at a scanning rate of  $0.02^\circ/s$  in a  $2\theta$  range of  $5\text{--}40^\circ$  on a Rigaku D/MAX 2580VB X-ray diffractometer with high-intensity Cu  $K\alpha$  radiation ( $\lambda = 0.154056\text{ nm}$ , Rigaku Corp., Tokyo, Japan).

## RESULTS AND DISCUSSION

### Determination of molar substitution (MS) for LSHEC

MS of LSHEC is the average number of moles of substituent groups per anhydroglucose unit,<sup>14</sup> and it is extremely significant for LSHEC solubility and fiber formation. MS of LSHEC was determined as reported.<sup>12</sup> Acetylation of both unsubstituted hydroxyl groups on anhydroglucose units and those at substituent end hydroxyl groups of LSHEC can eliminate spectral complications arising from hydrogen bonding. Figure 1 shows FTIR spectra of LSHEC and acetylated LSHEC. The strong absorption located at 3584, 3200, and 2890  $cm^{-1}$  for hydroxyl groups of LSHEC disappeared along with the presence of ester absorption at 1750 and 1240  $cm^{-1}$  for acetylated LSHEC, and this ensured nearly complete acetylation of the hydroxyl groups in LSHEC. The  $^1H$ -NMR spectrum of acetylated LSHEC is shown in Figure 2. MS of LSHEC was calculated to be 0.49 by the correlation of integrals of signals of anhydroglucose

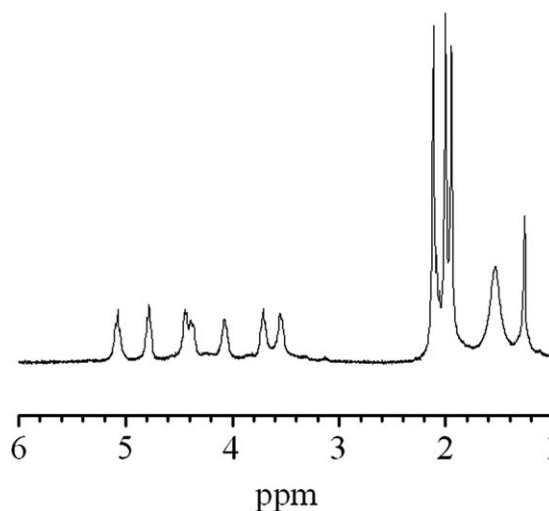


**Figure 2**  $^1H$ -NMR spectrum of acetylated LSHEC in  $CDCl_3$  at 40°C.

protons (5.1–2.9 ppm) with those of acetate moieties (2.1–1.9 ppm).<sup>15</sup> It was impossible to obtain a stable concentrated LSHEC spinning solution because of the poor solubility of LSHEC with MS lower than 0.5 in the alkali aqueous solution. However, a higher concentration of the spinning solution would provide LSHEC fibers with advantageous mechanical properties because of the densely packed and homogeneous interior fiber structures. In contrast, MS of LSHEC greater than 0.5 really improved its solubility but resulted in excessively swollen fibers with very low wet tensile strength even after coagulation. LSHEC suitable for spinning has an optimal MS value of about 0.5 according to our experimental results. An approximately 8.0 wt % concentration of the LSHEC spinning solution is comparable to that of viscose rayon, and this makes the fiber spinning of LSHEC facile because of the use of spinning processes and devices identical to those for viscose rayon.

### Rheology of the LSHEC spinning solutions

Dynamic rheology is a sensitive probe for studying the gel formation of LSHEC and can provide precise identification of the gel point during a gelation process.  $G'$  and  $G''$  are sensitive to the microstructures of LSHEC in the spinning solutions. Therefore,  $G'$  and  $G''$  can be used effectively to determine the gelation mechanism and kinetics. Gelation usually originates from the occurrence of three-dimensional network formation in a polymeric solution or melt. It is taken as the instant at which a system loses fluidity as measured by the failure of an air bubble to rise in it. Here the gel points of the LSHEC spinning solutions were defined alternatively as the crossover points of the shear moduli,  $G'$  and  $G''$ , based on rheological criteria.<sup>16–18</sup>

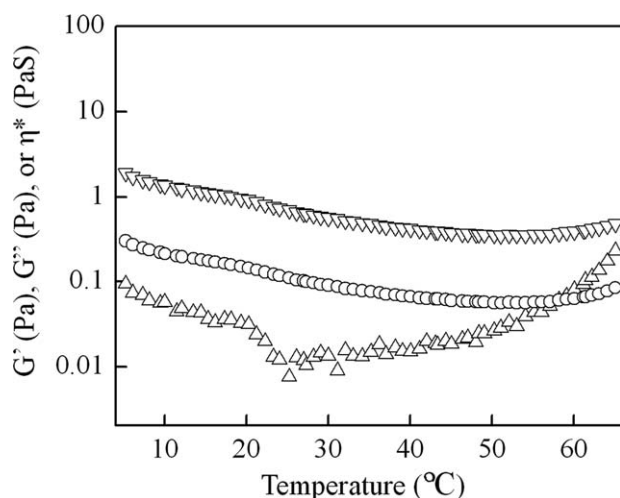


**Figure 3** Dependence of ( $\Delta$ )  $G'$ , ( $\nabla$ )  $G''$ , and ( $\circ$ )  $\eta^*$  of a 6.0 wt % LSHEC NaOH aqueous solution on elevated temperatures at a heating rate of 2°C/min.

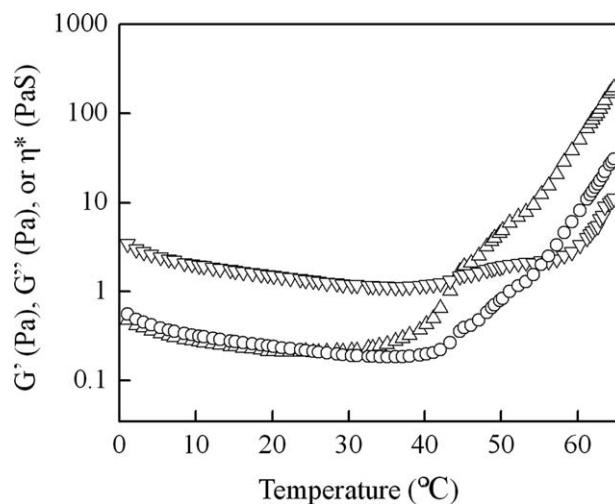


**Figure 4** Dependence of ( $\Delta$ )  $G'$ , ( $\nabla$ )  $G''$ , and ( $\circ$ )  $\eta^*$  of a 6.5 wt % LSHEC NaOH aqueous solution on elevated temperatures at a heating rate of 2°C/min.

At a constant concentration of the LSHEC spinning solution, the highest temperature still suitable for conducting a spinning process is designated the gelation onset temperature ( $T_{\text{gel}}$ ), which is identical to the temperature at the gel point featuring  $G' = G''$ . Figure 3–8 depict the variation of  $G'$ ,  $G''$ , and  $\eta^*$  with temperature for spinning solutions with different LSHEC concentrations. The viscoelastic properties of the LSHEC spinning solutions depended on their LSHEC concentrations because the spinning solutions exhibited an evolution from viscous properties to elastic properties with their concentrations ranging from 6.0 to 8.8 wt %. Therefore, the concentrations of the LSHEC NaOH aqueous solutions played a key role in their flow behaviors. Within the

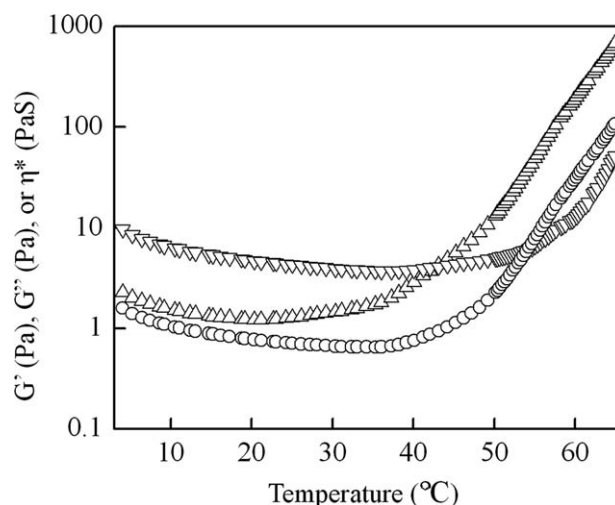


**Figure 5** Dependence of ( $\Delta$ )  $G'$ , ( $\nabla$ )  $G''$ , and ( $\circ$ )  $\eta^*$  of a 7.07 wt % LSHEC NaOH aqueous solution on elevated temperatures at a heating rate of 2°C/min.

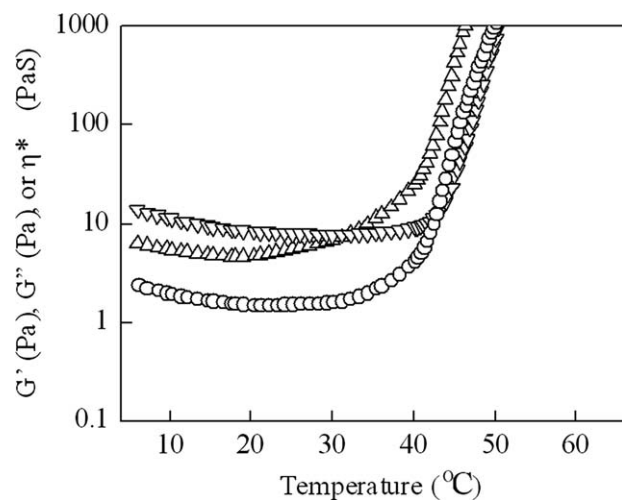


**Figure 6** Dependence of ( $\Delta$ )  $G'$ , ( $\nabla$ )  $G''$ , and ( $\circ$ )  $\eta^*$  of a 7.6 wt % LSHEC NaOH aqueous solution on elevated temperatures at a heating rate of  $2^\circ\text{C}/\text{min}$ .

whole range of measurement temperatures, the LSHEC NaOH aqueous solution with the concentration of 6.0 wt % behaved like a viscous fluid ( $G'' > G'$ ), whereas the solution with the concentration of 8.8 wt % lost its fluidity ( $G' > G''$ ) because of the formation of an elastic gel. Apart from these two solutions, gel was formed at  $G' = G''$  for the LSHEC NaOH aqueous solutions with LSHEC concentrations ranging from 6.5 to 8.2 wt %. Moreover, no equilibrium  $G'$  or  $G''$  was obtained during the temperature sweep for each viscoelastic LSHEC NaOH aqueous solution. The difference between  $G'$  and  $G''$  increased with the concentration after the gel points, and this suggested that the LSHEC hydrogel was reinforced at a higher concentration. At a definite LSHEC concentration, the difference between  $G'$  and

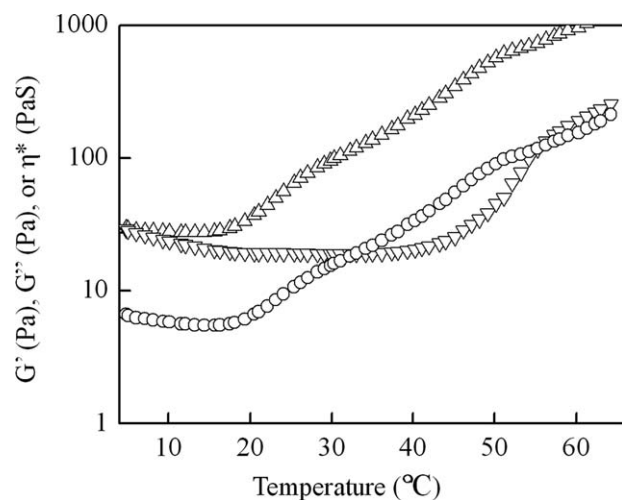


**Figure 7** Dependence of ( $\Delta$ )  $G'$ , ( $\nabla$ )  $G''$ , and ( $\circ$ )  $\eta^*$  of an 8.2 wt % LSHEC NaOH aqueous solution on elevated temperatures at a heating rate of  $2^\circ\text{C}/\text{min}$ .

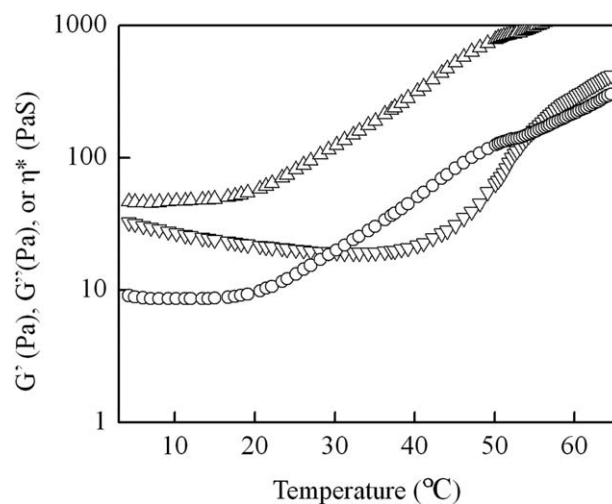


**Figure 8** Dependence of ( $\Delta$ )  $G'$ , ( $\nabla$ )  $G''$ , and ( $\circ$ )  $\eta^*$  of an 8.8 wt % LSHEC NaOH aqueous solution on elevated temperatures at a heating rate of  $2^\circ\text{C}/\text{min}$ .

$G''$  increased with the temperature above  $T_{\text{gel}}$ , and this indicated that the LSHEC hydrogel became stronger with the elevated temperature, and hence the hydrogel formation was an endothermic process. No equilibrium  $G'$  or  $G''$  was attained within the range of the measurement temperatures. Therefore, a higher temperature above  $T_{\text{gel}}$  favored the formation of a more elastic hydrogel.

At a definite LSHEC concentration higher than 6.0 wt %, the LSHEC NaOH aqueous solutions exhibited obvious features of a viscous fluid under a temperature below  $T_{\text{gel}}$ . A further increase in the temperature above  $T_{\text{gel}}$  led to an initial increase in  $\eta^*$ , which corresponded to the generation of a weak hydrogel network without collapse, and a subsequent abrupt increase in  $\eta^*$ , which corresponded to the generation of a much stronger hydrogel network dominated by chain association that screened out the effect of the increased temperature. Similarly, the LSHEC concentration also had a great impact on  $\eta^*$ . It was demonstrated again that the hydrogel networks were reinforced by the enhancement of either the temperature or the LSHEC concentration; this is illustrated more clearly later.

Figure 9 shows that the storage and viscous moduli at the gel points [the gelation modulus ( $G_{\text{gel}}$ )] increased with the concentrations of the LSHEC spinning solutions, indicating that a higher LSHEC concentration led to a stronger hydrogel with better mechanical properties. On the other hand,  $T_{\text{gel}}$  decreased with the concentrations of the spinning solutions, and this meant that a higher concentration favored the onset of gelation at a lower temperature because the dissolution of LSHEC was exothermic.  $\eta^*$  corresponding to the gel points increased with the LSHEC concentration, as shown in Figure 10,

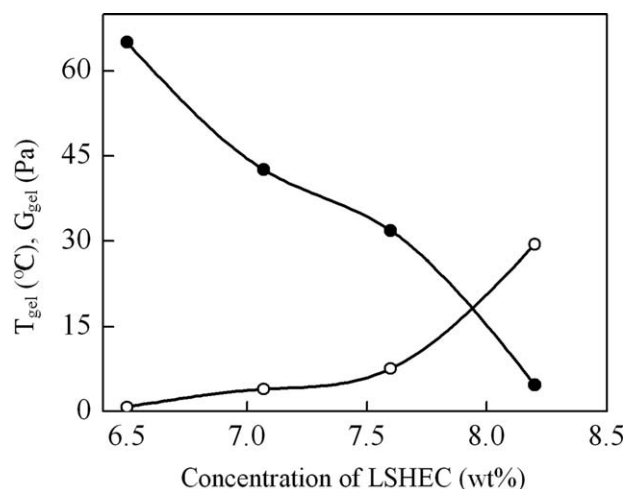


**Figure 9** (●)  $T_{gel}$  and (○)  $G_{gel}$  as functions of the LSHEC concentration for LSHEC NaOH aqueous solutions.

but  $\eta^*$  at the gel points was still very low in comparison with that of the hydrogels above  $T_{gel}$ .

#### Spinnability of the LSHEC NaOH aqueous solutions

From Figures 4–7, four pairs of spinning solution concentrations and  $T_{gel}$  values could be made, as depicted in Figure 11. A gelation onset curve was thus obtained by connection of the four points, and it denoted concentration–temperature combinations corresponding to the onset of gelation. The gelation onset curve could be extrapolated with more experimental results. A series of horizontal isoconcentration lines intersected with the gelation onset curve. The points at the intersections, or gelation points, could afford various combinations of the concentrations of the spinning solutions and spinning temperatures for the onsets of gelation or the spinnable lim-

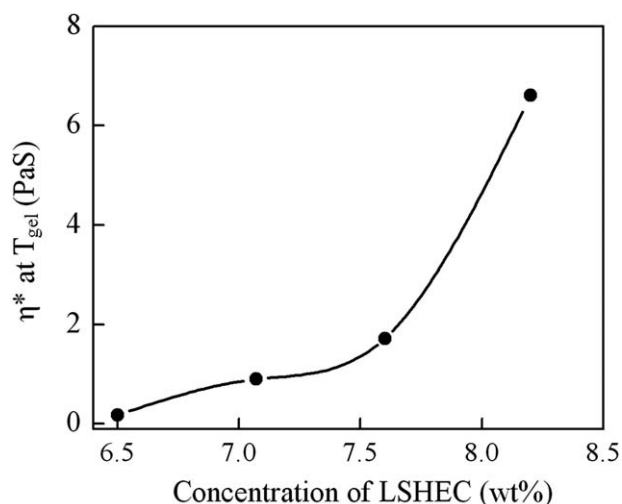


**Figure 10** Dependence of  $\eta^*$  at gel points on the LSHEC concentration for LSHEC NaOH aqueous solutions.

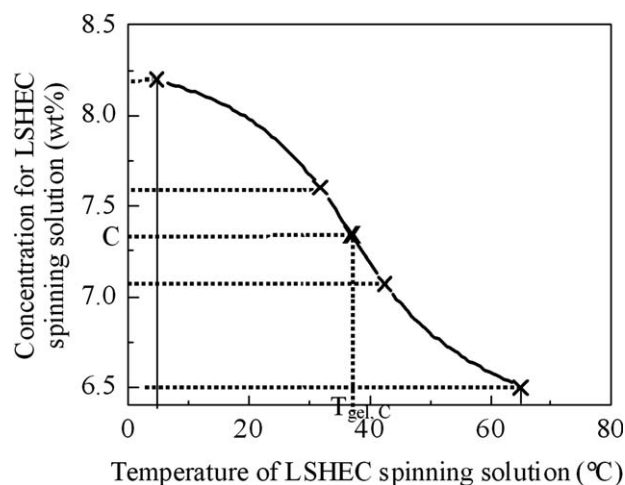


**Figure 11** Rheological gelation point as a function of the concentration and temperature of the LSHEC spinning solution.

its of the concentrations of the LSHEC spinning solutions and corresponding spinning temperature. At constant LSHEC concentration  $C$ , as shown in Figure 11, the highest temperature still suitable for conducting a spinning process is designated  $T_{gel,C}$ . On the horizontal line with constant LSHEC concentration  $C$ , a point away from the gelation point corresponds to a viscous fluid state of the LSHEC solution. When the point moves toward the gelation point, which is equivalent to a temperature increase, the LSHEC solution approaches its gel point, and this confirms that the dissolution of LSHEC is an exothermic process. The combinations of  $C$  and  $T_{gel,C}$  could be used as criteria for the spinnability of LSHEC NaOH aqueous solutions. In the rectangular area confined by two vertical borderlines in Figure 11, each point below the gelation onset curve denotes a combination of the LSHEC concentration and spinning temperature, which represents a visco-dominant LSHEC NaOH aqueous solution with  $G'' > G'$ . This region demarcates the necessary concentration of the LSHEC spinning solutions and the corresponding spinning temperature based on the rheological results. A high LSHEC concentration of the spinning solution is propitious for high fiber output and a densely packed fiber superstructure formed in the coagulation bath. However, it will cause  $G'$  to increase and the fluidity of the spinning solution to deteriorate. To maintain good fluidity of the LSHEC spinning solution, a combination of a high LSHEC concentration and a low dissolution temperature is favored for fiber spinning. However, the dissolution of LSHEC and its fiber spinning under a low temperature require a long time to reach the equilibrium because of the LSHEC dissolution dynamics. Considering both the dissolution dynamics and thermodynamics, viscose fiber manufacturers generally

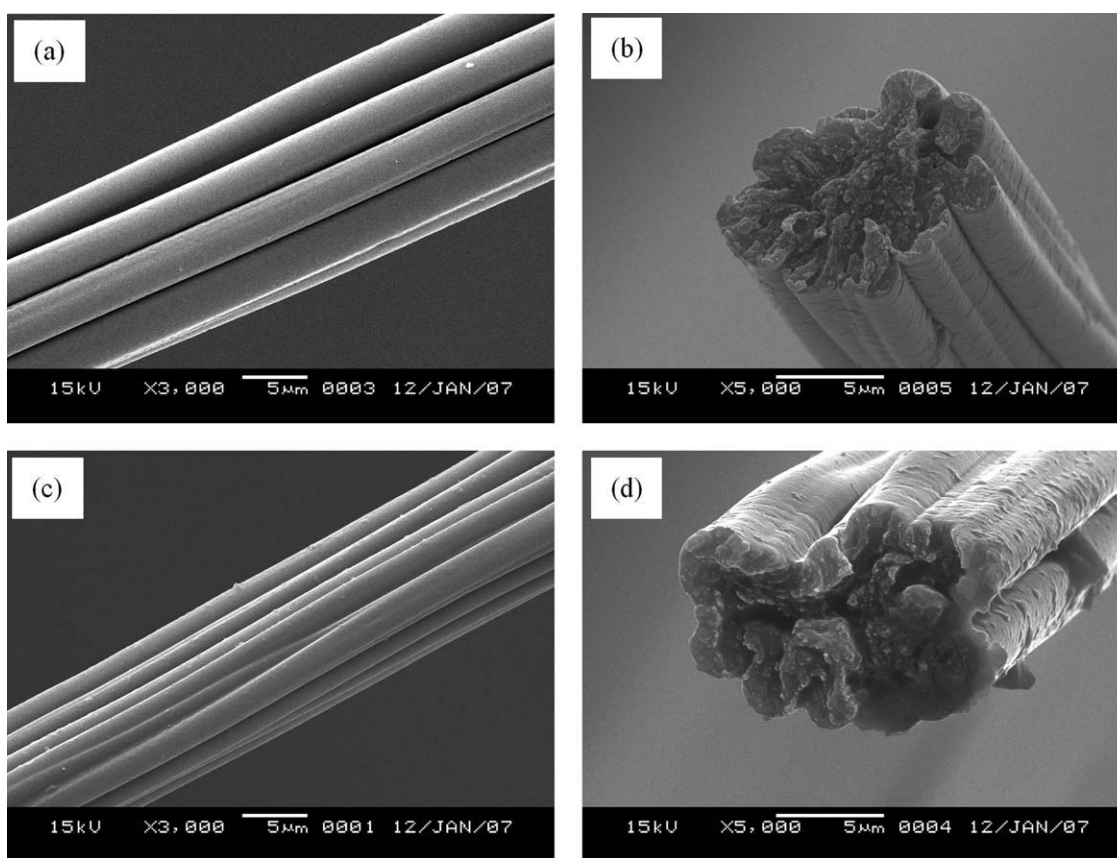


**Figure 12** SEM images of (a) LSHEC fibers in the direction of fiber axes, (b) cross section at the breakage of LSHEC fibers, (c) viscose rayon fibers in the direction of fiber axes, and (d) cross section at the breakage of viscose rayon fibers.

choose dissolution and spinning temperatures ranging from 20 to 25°C. Therefore, the optimal LSHEC concentration of the spinning solution can be selected from Figure 11 (e.g., 7.5–8.0 wt %). In contrast, each point above the gelation onset curve represents an elastic-dominant LSHEC gel with  $G' > G''$ . Although these points above the gelation onset curve are unable to offer appropriate spinning conditions, they practically provide rheological information on the temperature of the coagulation bath needed to achieve sufficiently strong hydrogels for subsequent fiber coagulation and multistep drawing. For the isoconcentration line with LSHEC concentration  $C$ , the temperature of the coagulation bath could be 40–60°C or, more appropriately, 50–60°C. The composition of the coagulation bath cannot be determined from Figure 11; it is generally determined thermodynamically from a polymer–solvent–precipitant ternary phase diagram.

#### LSHEC fibers

On the basis of the gelation onset curve in Figure 11, the dissolution temperature of LSHEC was selected to be 20°C. The spinning temperature for the spinning solution with the LSHEC concentration of

7.6 wt % was 25°C, and the temperature of the coagulation bath was 45°C. The as-spun LSHEC fibers had smooth surfaces [Fig. 12(a)] in the direction of the fiber axes, and they were similar to the surfaces of the viscose rayon fibers spun under identical conditions (concentration and temperature) associated with the same coagulation conditions, as shown in Figure 12(c). No remarkable disparity was observed from the SEM images of the cross sections at breakage for both the LSHEC and viscose rayon fibers. The dry tensile strength of the LSHEC fibers was 1.59 cN/dtex, and the wet tensile strength was 0.47 cN/dtex. The ratio of the wet tensile strength to the dry tensile strength was 0.30 for the LSHEC fibers. However, this value was approximately 0.5 for viscose rayon fibers supplied by Nanjing Chemical Fiber with dry and wet tensile strengths of 2.1 and 1.1 cN/dtex, respectively.<sup>11</sup> Therefore, it is still desirable to improve both the dry and wet tensile strengths of the LSHEC fibers (particularly the wet tensile strength) to increase the ratio of the wet tensile strength to the dry tensile strength to as much as approximately 0.5 via intrafiber chemical crosslinking by poly(carboxylic acid)s, as we reported.<sup>19,20</sup> The XRD pattern of the LSHEC fibers in Figure 13 shows the presence of a small

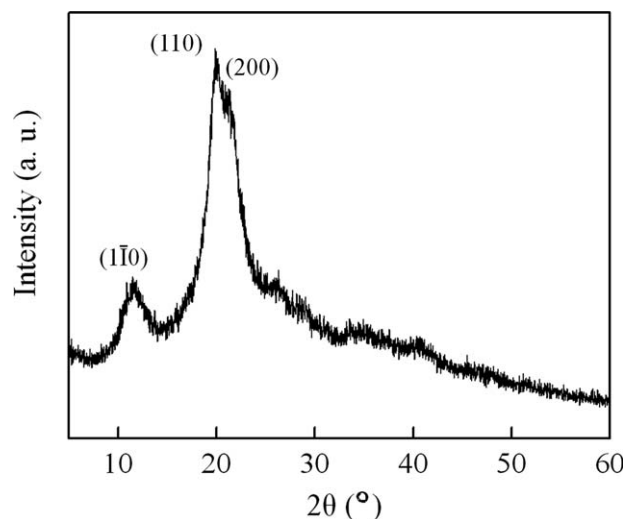


**Figure 13** XRD pattern of LSHEC fibers with MS = 0.49.

diffraction peak at  $2\theta = 11.56^\circ$  and double peaks at  $2\theta = 20.0^\circ$ , corresponding to the lattice planes of  $(1\bar{1}0)$ ,  $(110)$ , and  $(200)$  of cellulose II<sup>4</sup> and hydrate cellulose, respectively. The crystallinity of the LSHEC fibers was 57.8%, as determined from the XRD pattern. Accordingly, the crystallization behavior of the LSHEC fibers was similar to that of the viscose rayon fibers.<sup>4,11</sup> The low substitution degree of LSHEC did not alter the distinct crystallization behavior of the regenerated cellulose fibers.

### CONCLUSIONS

Ethylene oxide was used to etherify alkali cellulose with a low substitution degree to generate LSHEC, particularly for the purpose of avoiding the consumption of toxic CS<sub>2</sub>. The dissolution of LSHEC in NaOH aqueous solutions was an exothermic process, whereas the gelation of LSHEC was an endothermic process. The viscoelasticity of the LSHEC spinning solutions depended greatly on the LSHEC concentration and temperature. The gelation onset curve provided significant information on the spinnability of LSHEC, such as the spinning and coagulation conditions and the concentration–temperature combinations for both the spinning solutions and coagulation bath.

The LSHEC fibers were spun under the spinning conditions based on the rheological gelation onset

curve. The dry tensile strength of the LSHEC fibers was 1.59 cN/dtex, and the wet tensile strength was 0.47 cN/dtex. The ratio of the wet tensile strength to the dry tensile strength was 0.30, lower than that of commercially available rayon fibers. The primary reason for the low ratio of the wet tensile strength to the dry tensile strength was the low wet tensile strength due to the wet, swollen LSHEC fibers. Therefore, successive chemical crosslinking of the LSHEC fibers can possibly solve this problem by enhancing the wet and dry tensile strengths as well as the ratio of the wet tensile strength to the dry tensile strength to approximately 0.5 because the swollen degree of the LSHEC fibers could be diminished considerably by crosslinked intrafiber structures according to our recent research.<sup>19,20</sup>

### References

1. Yin, C.; Li, J.; Xu, Q.; Peng, Q.; Liu, Y.; Shen, X. *Carbohydr Polym* 2007, 67, 147.
2. Edgar, K. J.; Buchanan, C. M.; Debenham, J. S.; Rundquist, P. A.; Seiler, B. D. *Prog Polym Sci* 2001, 26, 1605.
3. Fink, H.-P.; Weigel, P.; Purz, H. J.; Ganster, J. *Prog Polym Sci* 2001, 26, 1473.
4. Cai, J.; Zhang, L.; Zhou, J.; Li, H.; Chen, H.; Jin, H. *Macromol Rapid Commun* 2004, 25, 1558.
5. Franks, N. E.; Varga, J. K. U.S. Pat. 4,196,282 (1980).
6. Gannon, J. M.; Graveson, I.; Mortimer, S. A. U.S. Pat. 5,725,821 (1998).
7. Urbanowski, A. *Chem Fibers Int* 1996, 46, 260.
8. Yin, C.; Shen, X. *Eur Polym J* 2007, 43, 2111.
9. Dönges, R. *Brit Polym J* 1990, 23, 315.
10. Kotseva, K.; Braeckman, L.; Duprez, D.; De Bacquer, D.; De Buyzere, M.; Van De Veire, N.; Vanhoorne, M. *Occup Med* 2001, 51, 223.
11. Shim, W. S.; Kim, J. P.; Lee, J. J.; Koh, J.; Kim, I. S. *Fiber Polym* 2008, 9, 691.
12. Tezuka, Y.; Imai, K.; Oshima, M.; Chiba, T. *Macromolecules* 1987, 20, 2413.
13. Tezuka, Y.; Imai, K.; Oshima, M.; Chiba, T. *Polymer* 1989, 30, 2288.
14. Zhou, J.; Qin, Y.; Liu, S.; Zhang, L. *Macromol Biosci* 2006, 6, 84.
15. Schaller, J.; Heinze, T. *Macromol Biosci* 2005, 5, 58.
16. Grillet, A. C.; Galy, J.; Pascault, J. P.; Bardin, I. *Polymer* 1989, 30, 2094.
17. Cheng, K. C.; Chiu, W. Y.; Hsieh, K. H.; Ma, C. C. M. *J Mater Sci* 1994, 29, 887.
18. Boey, F. Y. C.; Qiang, W. *J Appl Polym Sci* 2000, 76, 1248.
19. Li, W.; Zhao, X.; Chen, S.; Zhou, X.; Chen, D.; Wang, X. *Carbohydr Polym* 2008, 73, 223.
20. Li, W.; Xu, X.; Chen, S.; Zhou, X.; Li, L.; Chen, D.; Wang, X. *Carbohydr Polym* 2008, 71, 574.